The 4th International Symposium - Supercritical CO2 Power Cycles
September 9-10, 2014, Pittsburgh, Pennsylvania

STEADY-STATE POWER OPERATION OF A SUPERCRITICAL CARBON DIOXIDE BRAYTON CYCLE

E. M. Clementoni
Bechtel Marine Propulsion Corporation
West Mifflin, PA, USA
eric.clementoni@unnpp.gov

T. L. Cox
Bechtel Marine Propulsion Corporation
West Mifflin, PA, USA
timothy.cox@unnpp.gov

ABSTRACT

Bechtel Marine Propulsion Corporation (BMPC) is testing a supercritical carbon dioxide (S-CO_2) Brayton system at the Bettis Atomic Power Laboratory. The Integrated System Test (IST) is a two shaft recuperated closed Brayton cycle with a variable speed turbine drive compressor and a constant speed turbine driven generator using S-CO_2 as the working fluid designed to output 100 kWe. The main focus of the IST is to demonstrate operational, control and performance characteristics of an S-CO_2 Brayton power cycle over a wide range of conditions.

IST operation has been limited in power level due to issues with the permanent magnet rotor and motor-generator controller for the turbine-generator. Remagnetization of the rotor along with motor-generator controller improvements have increased the power output capability of the generator to at least 40 kWe. Steady-state operation at various power levels from near zero net system power to maximum operating power of 40 kWe is presented.

INTRODUCTION

The S-CO_2 Brayton cycle is being actively developed for potential application in a wide range of energy conversion applications. S-CO_2 Brayton system development efforts at BMPC have primarily been focused on system thermodynamics, system control modeling, and the design, construction, and testing of the 100 kWe Integrated System Test (IST) [1-4].

The IST is a simple recuperated closed loop S-CO_2 Brayton system with a variable speed turbine-compressor and a constant speed turbine-generator (Figure 1). The IST is designed to generate nominally 100 kWe at a relatively modest turbine inlet temperature of 570°F (299°C) as shown in the design full power heat balance (Figure 2). Due to the small scale of the IST equipment, overall loop efficiency is much lower than is predicted for larger S-CO_2 Brayton cycles.

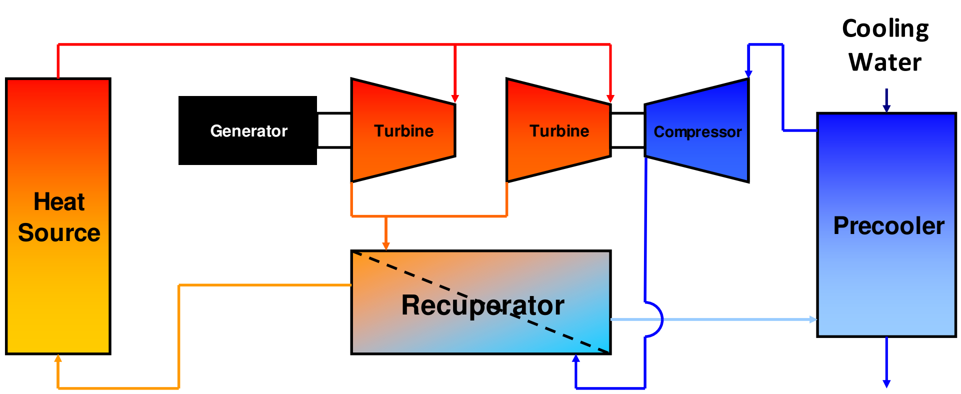

Figure 1. Simple Recuperated Brayton Cycle

The IST component layout is shown in Figure 3, and Figure 4 shows the physical arrangement of the test loop. The heat source for the IST is a 1 MW electrically heated organic heat transfer fluid system which transfers heat to the CO_2 through a standard shell-and-tube heat exchanger. The heat sink is a chilled water system which rejects heat from the precooler and other heat loads to a refrigerated chiller. This chilled water system is broken into two loops so that cooling flow can always be provided to auxiliary heat loads throughout the system while the precooler can either be cooled from this chilled loop or heated during startup through a separate water loop to achieve supercritical conditions in the CO_2.

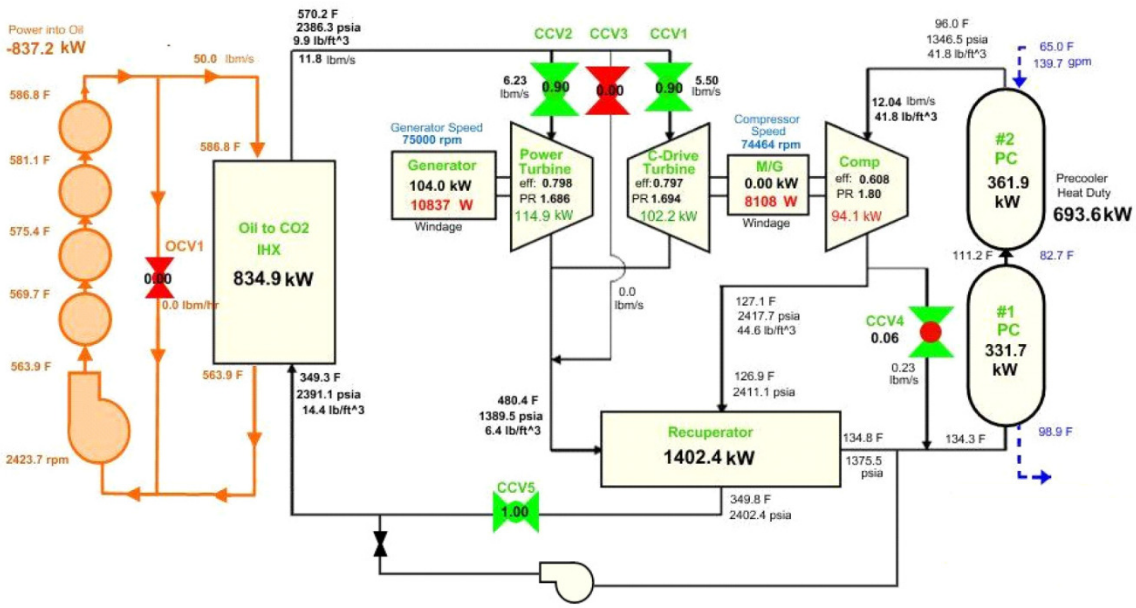

Figure 2. IST Design Full Power Heat Balance

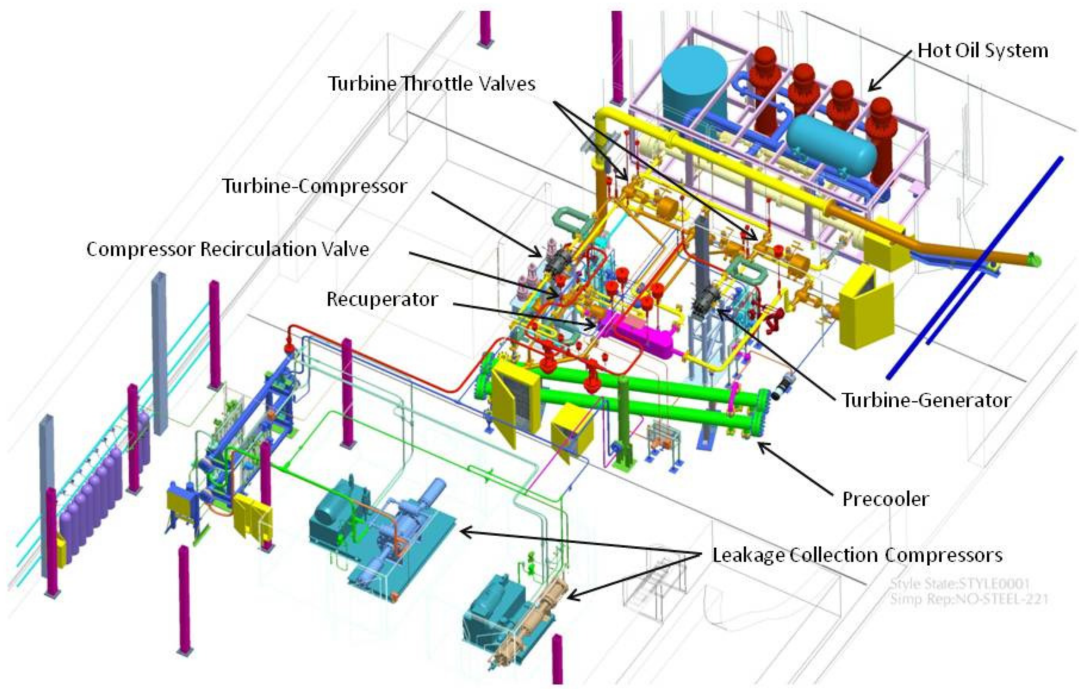

Figure 3. IST Component Arrangement

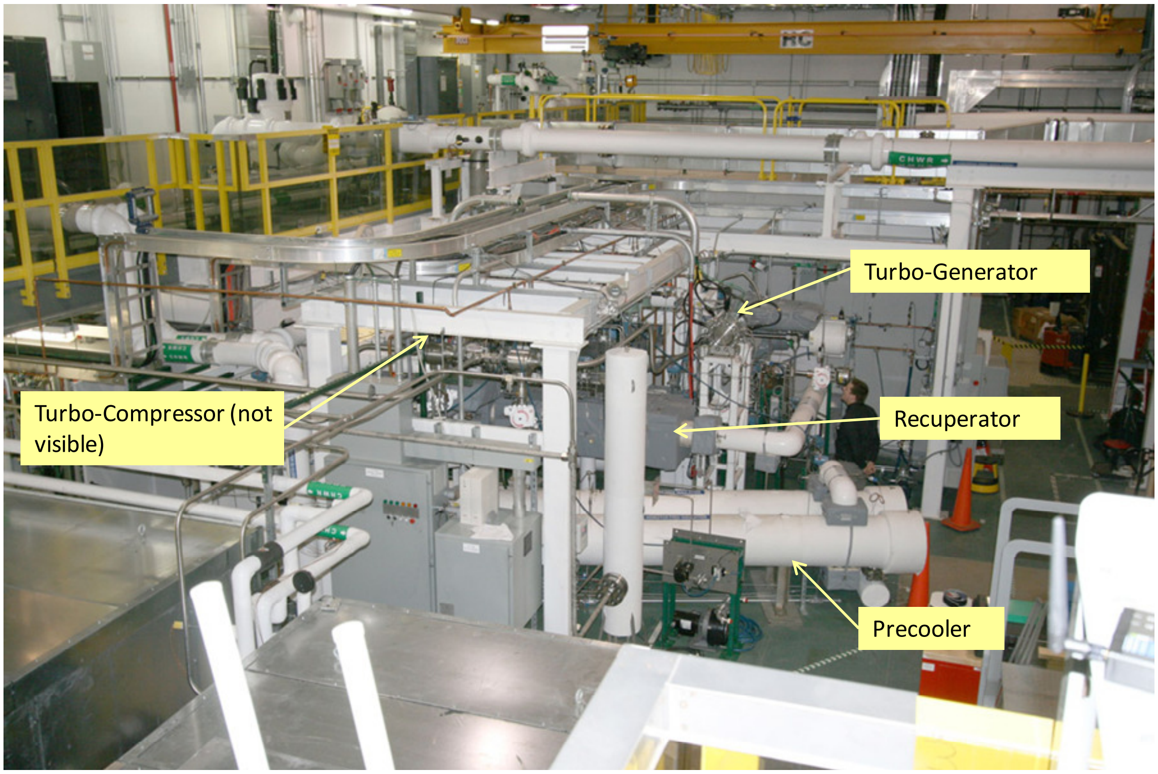

Figure 4. IST Physical Layout

SYSTEM OPERATIONAL OVERVIEW

A full description of system startup and operation is provided in [5]; for easy reference, the primary steps are repeated here. The IST is started by first warming the system and adjusting system CO_2 mass to achieve the desired temperatures and pressures to achieve supercritical conditions throughout the entire main Brayton loop and promote forward flow through the turbines during startup. The turbine-compressor and turbine-generator are sequentially started by motoring them to an idle speed of 37,500 rpm. The system is then heated to normal operating temperature by increasing the heater temperature setpoint at a defined rate. Compressor inlet temperature is maintained at 96°F (36°C) by automatic feedback control of the cooling water flow rate through the precooler. Compressor inlet pressure varies as the power level is changed due to a change in the mass distribution in the main loop and the sub-system which maintains turbomachinery motor-generator cavity pressure. This mass redistribution is created by a change in the temperature and density profiles of the CO_2 in the main loop and in the turbine-compressor motor-generator cavity as the shaft speed changes.

The IST control system and operating conditions were designed such that the compressor recirculation valve (CCV4) is set at 6% open (minimum flow position) at maximum system power. Ideally, this valve would be fully closed at maximum system power, but the hysteresis band of the installed valve could cause system instability if it is operated below 6% open. The system operating conditions are being chosen to achieve maximum power with the compressor recirculation valve at minimum position. The turbine and main loop throttle valves remain fully open throughout normal operation.

IST shakedown and low power operation utilized control system parameters developed with the transient IST system model developed by BMPC using as-designed component information [6-7]. This testing exploited the motor-generator capability of each turbomachine to either motor or load the shafts as necessary to maintain the turbine-compressor and turbine-generator at the commanded shaft speeds. As a result of differences between as-designed and as-built component performance, the turbine-compressor was always motored to maintain the commanded shaft speed during this initial phase of testing.

IST operation has progressed to the point where the turbine-compressor has been operated in a thermal-hydraulically balanced state where the power produced by the turbine is equal to the power consumed by the compressor and rotor windage losses. Initial testing with the turbine-compressor thermal-hydraulically balanced has been performed with the turbine-generator operating at 60,000 rpm rather than the design speed of 75,000 rpm [8]. Once the turbine-compressor is operating in a thermal-hydraulically balanced state, the power level of the turbine-generator is changed by modulating the compressor recirculation valve (CCV4). Automatic feedback control of the heaters maintains the CO_2 temperature at the outlet of the intermediate heat exchanger at the setpoint turbine inlet temperature.

IST POWER LIMITATIONS

The maximum power output of the IST has been limited due to issues with the turbine-generator motor-generator controller. The motor-generator controller determines the position of the rotor by sensing the voltage output of a separate coil embedded in the stator of the machine. As the system power level is increased, the generator output voltage begins to decline which also causes the voltage waveform used for rotor position indication to become smaller. The position indication algorithm currently does not include compensation for voltage degradation and the position indication begins to experience a phase shift because the position signal does not cross the threshold voltage until later in the waveform. This shift causes the firing of the power electronics in the controller to gradually lag the desired state causing an increasing phase angle in the generator output current waveform with respect to the voltage waveform. Thus the power factor degrades requiring more current to achieve the same power which thereby causes further voltage reduction until the point where the phase shift has gotten too large for the controller to pass the necessary currents and speed control is lost.

In order to reduce the voltage droop with power level, the permanent magnet rotor was remagnetized. It was believed that the magnets were not initially magnetized to saturation which was further exacerbating the voltage degradation. Initial testing at low power indicated an improved generator output voltage which led to additional testing to determine the improvement in system output power capability.

RESULTS

Testing was performed with a turbine inlet temperature of 540°F (282°C) and a turbine-generator speed of 55,000 rpm. The turbine-compressor speed was initially set to 37,500 rpm which resulted in both shafts being motored to maintain the desired speed setpoint. The turbine-compressor speed was then raised to 45,000 rpm with a corresponding automatic reduction in compressor recirculation valve position. Due to differences in the as-tested conditions compared to the as-built model, the turbine-compressor was still motoring at low power through the entire test but the turbine-generator was generating more power than the turbine-compressor was consuming. The turbine-compressor speed was incrementally increased to 55,000 rpm in 1,000 rpm steps with the system being allowed to stabilize between steps. A Yokogawa WT1800 Power Analyzer was used to directly measure the AC power output from the generator for comparison to the DC power measured and reported by the motor-generator controller. Figure 5 shows the individual turbomachine powers along with the net Brayton power and cycle efficiency as the compressor speed is increased. Steady-state operating data for the system and two turbomachines is provided in Table 1.

The maximum turbine-generator power level achieved was 40 kW AC as measured with the Yokogawa Power Analyzer or 31 kW DC as reported by the motor-generator controller. The maximum steady-state power achieved prior to the rotor remagnetization was 24 kW DC indicating at least 29% improvement in the output power capability of the turbine-generator due to remagnetization of the rotor. The heat balance for the maximum power operating condition is shown in Figure 6. The Yokogawa Power Analyzer consistently indicated an AC power that was approximately 25% greater than the DC power reported by the motor-generator controller. This difference could be caused by AC-to-DC conversion losses, inaccurate measurement of the high switching frequency DC power by the controller, or a combination of the two.

Overall system performance matched very well with transient model predictions. While the turbomachine powers do not agree with predictions due to higher than modeled windage losses, the rest of the system performed much as expected. Figure 7 shows the calculated compressor performance on the compressor map supplied by the turbomachinery manufacturer. Test data is shifted to the right on the map compared to model predictions since the model predictions were performed at the design turbine inlet temperature of 570°F (299°C) and turbine-generator speed of 75,000 rpm. However, the trend in the data matches suitably with the predictions.

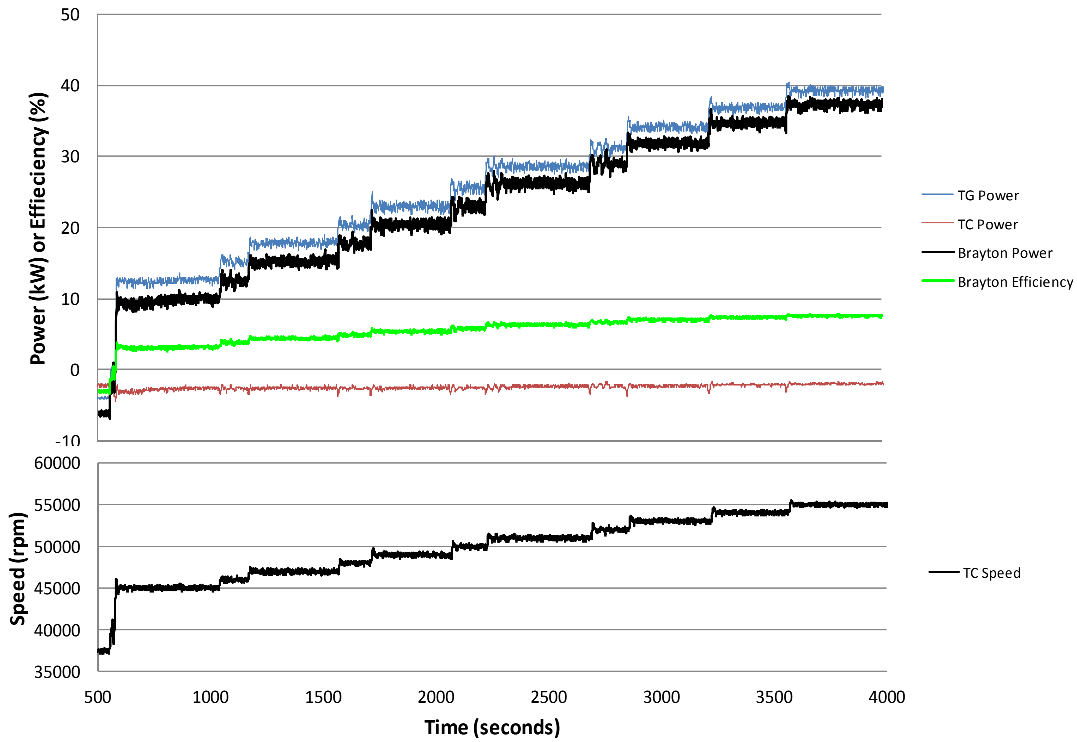

Figure 5. System Powers and Turbine-Compressor Speed

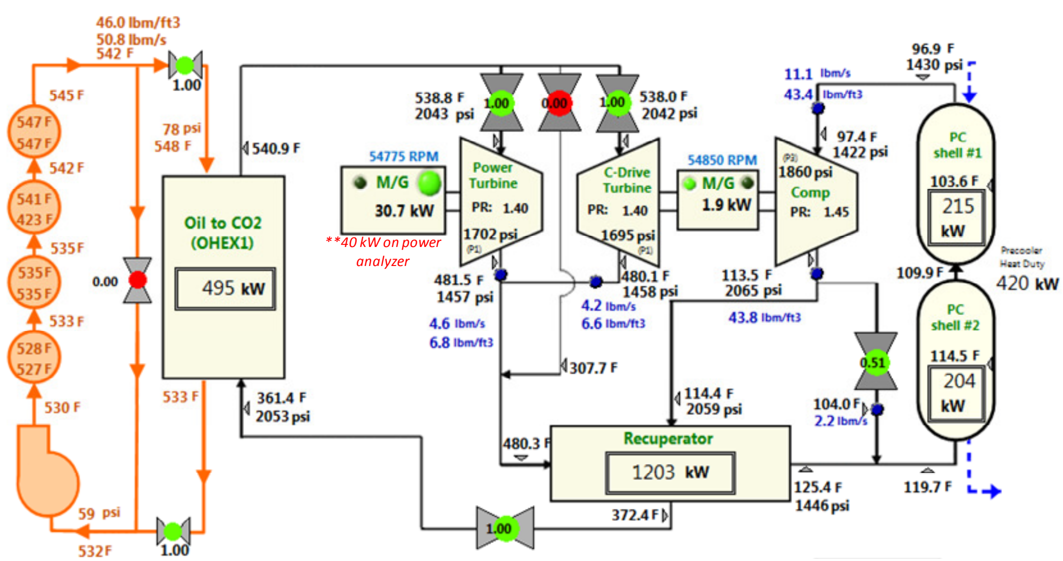

Figure 6. Heat Balance for Maximum Power Operating Condition

Table 1. Steady-State Operating Data

Net Brayton Power (kW)	-5.9	10.4	12.3	15.6	17.9	20.7	23.7	27.1	29.7	32.8	35.6	37.6
IHX Heat Transfer to CO_2 (kW) *[Calculated]*	205.8	318.0	331.6	352.8	366.4	385.0	402.6	420.9	440.7	458.0	478.3	497.2
Brayton Efficiency	-2.9%	3.3%	3.7%	4.4%	4.9%	5.4%	5.9%	6.4%	6.7%	7.2%	7.4%	7.6%
Compressor Recirculation Valve Position (% open)	70.4	62.2	61.4	60.3	59.0	58.1	57.0	55.9	54.9	53.5	52.2	51.0
Recuperator Duty (kW) *[Calculated]*	752.3	972.2	994.8	1025.3	1043.9	1073.5	1097.5	1117.3	1140.4	1157.8	1179.3	1202.6
Turbine-Generator Speed (rpm)	55000	55000	55000	55000	55000	55000	55000	55000	55000	55000	55000	55000
Generator Turbine Flow (lbm/s)	2.22	3.27	3.41	3.54	3.68	3.81	3.99	4.09	4.22	4.35	4.53	4.62
Generator Turbine Inlet Temperature (°F)	537.1	538.1	537.9	538.3	538.2	538.5	538.6	538.7	538.7	538.9	538.8	539.0
Generator Turbine Outlet Temperature (°F)	508.2	496.4	494.7	493.4	491.8	490.6	488.9	487.3	485.7	484.1	482.7	481.6
Generator Turbine Inlet Pressure (psia)	1658.8	1804.7	1822.3	1846.6	1869.8	1888.8	1913.9	1937.9	1961.4	1987.3	2012.9	2042.0
Generator Turbine Outlet Pressure (psia)	1400.7	1429.7	1431.6	1434.6	1441.1	1440.1	1443.5	1445.1	1446.5	1449.3	1451.5	1457.7
Turbine-Generator AC Power (kW)	-3.9	12.9	15.1	18.3	20.4	23.3	26.2	29.3	32.1	35.0	37.6	39.6
Turbine-Generator DC Power (kW)	-3.9	10.2	11.9	14.4	16.1	18.4	20.6	23.1	25.3	27.6	29.6	31.2
Turbine Power (kW) *[Calculated]*	14.3	30.4	32.8	35.3	37.8	40.2	43.5	46.0	48.8	51.9	55.0	57.2
Turbine-Generator Windage (kW) *[Calculated]*	18.2	17.5	17.7	17	17.4	16.9	17.3	16.7	16.7	16.9	17.4	17.6
Turbine-Compressor Speed (rpm)	37500	45000	46000	47000	48000	49000	50000	51000	52000	53000	54000	55000
Compressor Turbine Flow (lbm/s)	2.68	3.31	3.39	3.49	3.58	3.66	3.77	3.86	3.95	4.04	4.14	4.23
Compressor Turbine Inlet Temperature (°F)	536.4	537.2	537.1	537.5	537.4	537.7	537.8	537.9	537.9	538.1	538.1	538.2
Compressor Turbine Outlet Temperature (°F)	506.2	496.6	495.1	493.7	492.2	490.8	489.0	487.3	485.5	483.9	481.8	480.3
Compressor Turbine Inlet Pressure (psia)	1656.6	1802.7	1820.7	1844.9	1868.4	1887.2	1912.5	1936.3	1960.1	1986.1	2011.8	2040.9
Compressor Turbine Outlet Pressure (psia)	1401.4	1430.4	1432.2	1435.3	1441.9	1440.9	1444.3	1445.8	1447.0	1449.9	1452.1	1458.2
Compressor Flow (lbm/s)	7.81	9.29	9.50	9.73	9.85	10.09	10.29	10.47	10.68	10.83	10.99	11.16
Compressor Inlet Temperature (°F)	97.1	97.2	97.2	97.2	97.3	97.2	97.3	97.1	97.2	97.2	97.2	97.3
Compressor Outlet Temperature (°F)	104.6	107.9	108.4	108.9	109.5	109.9	110.6	111.1	111.6	112.1	112.8	113.4
Compressor Inlet Pressure (psia)	1382.8	1405.2	1406.2	1408.0	1413.8	1411.6	1413.9	1414.4	1414.5	1416.2	1417.2	1422.1
Compressor Outlet Pressure (psia)	1666.5	1818.2	1836.8	1862.0	1886.1	1905.8	1931.9	1956.6	1981.1	2007.9	2034.3	2064.2
Turbine Power (kW) *[Calculated]*	-2.0	-2.5	-2.8	-2.7	-2.5	-2.6	-2.5	-2.2	-2.4	-2.2	-2.0	-2.0
Compressor Power (kW) *[Calculated]*	18.3	29.8	31.5	33.7	35.6	37.6	40.3	42.6	45.0	47.7	50.6	53.1
Turbine-Compressor Windage (kW) *[Calculated]*	5.6	13.9	15.7	16.8	18.9	20.6	22.5	25.2	25.9	26.9	29.5	31.7

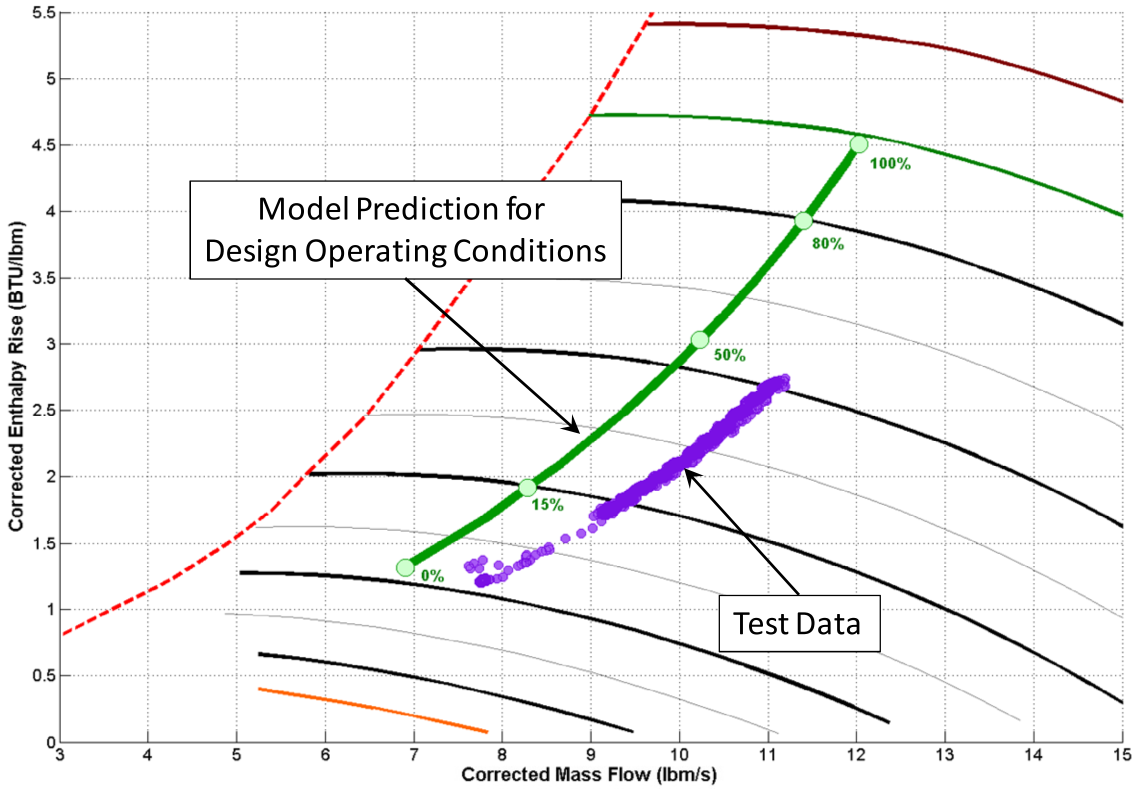

Figure 7. Compressor Map with Test Data and Model Predictions

A conservative maximum power criterion was used during this test to maintain the generator output current below the maximum steady-state current experienced before remagnetization to reduce the possibility of a loss of speed control. Further analysis of the test data indicates that the system could have been operated at higher power levels before reaching the point where speed control would have been lost. Additionally, a higher turbine-generator speed is planned to be used for future IST operations. The output voltage of the permanent magnet rotor is proportional to speed resulting in an increased power capability of the machine. Based on these factors, the maximum achievable power for the turbine-generator is predicted to be approximately 50 kW AC.

CONCLUSIONS

The IST continues to make progress in meeting its intended purpose of demonstrating controllability of the S-CO_2 Brayton cycle. The system has been operated to a maximum turbine-generator output power of 40 kWe with the expectation that approximately 50 kWe is achievable by operating at a higher speed and with less restrictive operating limits. The operating conditions for the loop have been modified based on this new maximum system power limit to maintain the objective of having the compressor recirculation valve at the minimum flow position at maximum system power. Testing through the full range of system power levels with the turbine-compressor operating in the thermal hydraulically balanced condition is planned to further demonstrate the controllability of the system.

The overall Brayton cycle has performed very closely to expectations for the operations performed to date. No inherent issues with the S-CO_2 Brayton cycle have been identified. Electrical issues with the motor-generator controllers and mechanical issues with gas foil thrust bearings have limited system operating power and the amount of testing that has been able to be accomplished. These issues are a result of using equipment that is not typical of what would be used in a larger system due to the small scale and high turbomachinery speed of the IST.

NOMENCLATURE

BMPC	=	Bechtel Marine Propulsion Corporation
IST	=	Integrated System Test
S-CO_2	=	Supercritical Carbon Dioxide

REFERENCES

[1] Ashcroft, J. A, Kimball, K. J., and Corcoran, M. R., "Overview of Naval Reactors Program Development of the Supercritical Carbon Dioxide Brayton System", *Proceedings of the Supercritical CO_2 Power Cycle Symposium*, Troy, NY, April 2009.

[2] Kimball, K. J., "Overview of Naval Reactors Program Development of the Supercritical Carbon Dioxide Brayton System," *Proceedings of the Supercritical CO_2 Power Cycle Symposium*, Boulder, CO, May 2011.

[3] Kimball, K. J. and Clementoni, E. M., "Supercritical Carbon Dioxide Brayton Power Cycle Development Overview," *Proceedings of ASME Turbo Expo 2012*, Copenhagen, Denmark, June 11-15, 2012.

[4] Kimball, K. J. and Clementoni, E. M., "Supercritical Carbon Dioxide Brayton Power Cycle Development Overview," *Proceedings of ASME Turbo Expo 2013*, San Antonio, Texas, USA, June 3-7, 2013.

[5] Clementoni, E. M., Cox, T. L., and Sprague, C. P., "Startup and Operation of a Supercritical Carbon Dioxide Brayton Cycle," *Journal of Engineering for Gas Turbines and Power*, Vol. 136, July 2014.

[6] Hexemer, M. J., Hoang, H. T., Rahner, K. D., Siebert, B., and Wahl, G. D., "Integrated Systems Test (IST) S-CO_2 Brayton Loop Transient Model Description and Initial Results", *Proceedings of the Supercritical CO_2 Power Cycle Symposium*, Troy, NY, April 2009.

[7] Hexemer, M. J., "Supercritical CO_2 Brayton Cycle Integrated System Test (IST) TRACE Model and Control System Design", *Proceedings of the Supercritical CO_2 Power Cycle Symposium*, Boulder, CO, May 2011.

[8] Clementoni, E. M. and Cox, T. L., "Steady-State Power Operation of a Supercritical Carbon Dioxide Brayton Cycle," *Proceedings of ASME Turbo Expo 2014*, Dusseldorf, Germany, June 16-20, 2014.